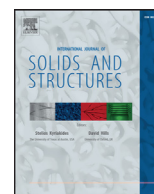




Contents lists available at ScienceDirect

## International Journal of Solids and Structures

journal homepage: [www.elsevier.com/locate/ijsolstr](http://www.elsevier.com/locate/ijsolstr)

## Perfectly matched layers for flexural waves: An exact analytical model

M. Morvaridi<sup>a</sup>, M. Brun<sup>b,\*</sup><sup>a</sup> Dipartimento di Ingegneria Civile ed Architettura, Università di Cagliari, Piazza d'Armi, 09123 Cagliari, Italy<sup>b</sup> Dipartimento di Ingegneria Meccanica, Chimica e dei Materiali, Università di Cagliari, Piazza d'Armi, 09123 Cagliari, Italy

## ARTICLE INFO

## Article history:

Received 20 May 2016

Revised 15 October 2016

Available online xxx

## Keywords:

Flexural waves

Geometric transformation

Perfectly matched layers

Cloaking

Harmonic analysis

Transient analysis

## ABSTRACT

In this paper we present an analytical model of Perfectly Matched Layers for flexural waves within elongated beam structures. The model is based on transformation optics techniques and it is shown to work both in time harmonic and transient regimes. A comparison between flexural and longitudinal waves is detailed and it is shown that the bending problem requires special interface conditions. A connection with transformation of eigenfrequencies and eigenmodes is given and the effect of the additional boundary conditions introduced at the border of the Perfectly Matched Layer domain is discussed in detailed. Such a model is particularly useful for Finite Element analyses pertaining propagating flexural waves in infinite domain.

© 2016 Elsevier Ltd. All rights reserved.

## 1. Introduction

In engineering applications the necessity to model unbounded domains is often required. This is particular important in modeling of soil-structure interaction (Lee and Tassoulas, 2011; Tassoulas and Kausel, 1983; Clouteau et al., 2013), fluid-solid interaction (Hu et al., 2016; Romero et al., 2015), ground-borne noise and vibration emitted by transportation systems (Clouteau et al., 2000; Steele, 2001), geophysics (Geli et al., 1988; Robinovich et al., 2011), non-destructive evaluation methods (Kim and Kim, 2009; Parvanova et al., 2014), fluid-dynamics and traffic flow (Lo and Wang, 2005) and general problems of wave propagation (electromagnetic, elastic, acoustics, seismic). The list includes also hydro- and aerodynamic problems (external flows, duct flows, reacting flows, jets, boundary layers, free surfaces with aerospace, marine/naval, automotive, meteorological, industrial and environmental applications), flows in porous media, filtration (with applications to oil recovery), magneto- hydrodynamic flows, plasma (e.g., solar wind) just to name a few.

In order to keep the computation feasible there is the necessity to truncate the models within a finite computational domain. This can be done by the boundary integral methods, infinite elements, non-reflecting boundary conditions and absorbing layers. The boundary element method (see, for example, the monographs (Bonnet, 1999; Wrobel, 2002; Aliabadi, 2002; Beer, 2001; Gaul et al., 2003)) can be used directly for exterior problems over a finite region.

It is an efficient numerical technique formulated for both static and dynamic problems, which is computationally cost effective in view of the fact that it reduces the dimensionality of the problem and only the boundary of the domain needs to be discretized. On the contrary, it is more difficult to implement with respect to Finite Element and Finite Difference algorithms and the coupling with different numerical schemes requires special attention. Also, some of the advantages of the method are lost and additional difficulties arise for non-linear problems in plasticity (Telles and Brebbia, 1979; Polizzotto, 1988; Maier et al., 1995; Bertoldi et al., 2005) and finite elasticity (Phan-Thien, 1988; Novati and Brebbia, 1982; Polizzotto, 2000; Brun et al., 2003a,b).

Infinite element schemes (Bettess and Zienkiewicz, 1977; Bettess, 1992) represent the domain in its entirety by using elements of infinite extent where the shape functions include outwardly propagating wave-like factors. The formulation may rely on a truncated multipole expansion (Burnett, 1994; Leis, 1986), that incorporates frequency dependent interpolation functions along the radial (outward) direction (Gerdes, 2000; Ihlenburg, 1998). However, infinite elements have problems of accuracy and unwanted boundary reflections in the case of the propagation of guided or bulk waves (Liu and Quek, 2003; Cremers and Fyfe, 1995; Astley and Hamilton, 2006). Also, a region much larger than the region of interest must be implemented in order to achieve accuracy.

Absorbing boundary conditions (ABCs) and perfectly matched layers (PMLs) permit outward propagating waves and must suppress spurious reflections at least to an acceptable level. ABCs were first introduced in Lysmer and Kuhlemeyer (1969), where it is shown that, for second order wave equations and linearized shal-

\* Corresponding author. Fax: +390706755418.  
E-mail address: [mbrun@unica.it](mailto:mbrun@unica.it) (M. Brun).

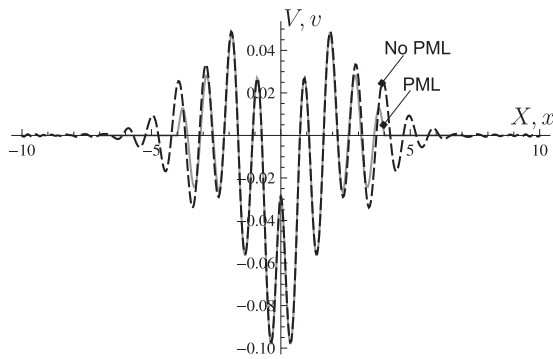


**Fig. 1.** Transient Finite Element analysis. Transverse displacement at  $t = 0.5$  s in a beam subjected to a transient force  $F(t)$  applied at  $X = 0$  m.  $F(t)$  is shown in Fig. 8. Dashed black line shows the displacement in a large domain without PMLs, continuous gray line shows the displacement in a short domain with PMLs.

low water equations, exact conditions are expressed in term of integro-differential equations which are then approximated by a hierarchical system of differential equations (Nataf, 2013).

Instead of ad-hoc boundary conditions PML is an area bordering the computational domain where waves are damped so that propagating waves become evanescent. The key property is always the absence of reflection at the interface between the physical and the absorbing domains. The problem of reflection at the interface between the physical domain and the absorbing one was solved in Berenger (1994) for problems governed by Helmholtz equations. The PMLs have become the most popular absorbing conditions for finite-difference time-domain and finite element wave simulations and many examples demonstrate their superior performance as compared to 'sponge-layer' absorbing boundary condition (Cerjan et al., 1985; Sochacki et al., 1987), paraxial conditions (Higdon, 1991; Quarteroni et al., 1998), asymptotic local or non-local operators (Givoli, 1991; Hagstrom and Hariharan, 1998).

PMLs correspond to a coordinate transformation in which the coordinate normal to the artificial boundary is mapped to complex values leading to decaying amplitude behavior (Chew and Weedon, 1994). They can be also interpreted as a viscous anisotropic material in the boundary region (Rappaport, 1996). It is highly effective in absorbing waves over wide ranges of frequency and incidence angles, is numerically stable and needs relatively thin layers. PML was first developed for electromagnetic waves (Berenger, 1994; Chew and Weedon, 1994), and then extended to the fields of acoustics (Qi and Geers, 1998), seismology (Komatitsch and Tromp, 2003; Kristek et al., 2009), dispersive waves (Lancioni, 2012) as well as to elastic waves (Hastings et al., 1996; Song et al., 2005; Nataf, 2005; Zheng and Huang, 2002). Surprisingly, applications to flexural waves, governed by fourth-order differential equations, are limited to a recent result, which is focused on the numerical implementation (Farzanian and Arbabi, 2014). The purpose of the work is to fill this gap.

In Chang et al. (2014) the construction of PMLs for elastic wave propagation was linked to conformal mapping techniques adopted for the design of invisibility cloaks (Milton et al., 2006; Brun et al., 2009; Norris and Shuvalov, 2011), a technique implemented in the numerical simulation given in Brun et al. (2009). Here we implement a similar approach for the problem of flexural waves (Brun et al., 2014a; Colquitt et al., 2014; Jones et al., 2015).

The model presented is studied in the time-harmonic regime. However, the simple computation given in Fig. 1 shows that the proposed PML performs well also in the transient regime. In the paper we compare the case of longitudinal and transverse waves within an elongated beam in order to stress the additional issues

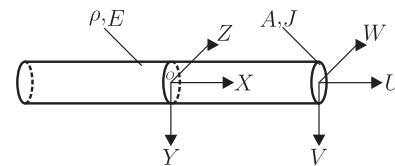


**Fig. 2.** Beam structure. The displacement at point  $X$  and time  $t$  is  $\mathbf{U} = (U, V, W)$ .

associated to the flexural case. Also, we give particular importance to the physical interpretation of the PML.

The structure of the paper is as follows. In Section 2 we present the transformation optics technique for longitudinal waves in a thin rod, we detail the transformed equation, we discuss the interface boundary conditions and present a comparison with the analytical Green's function in a infinite rod. In Section 3, we present the model for flexural waves in beam structures. We detail the transformed equation and we discuss the condition on the transformation in order to automatically satisfy interface conditions. We present different numerical examples concerning invariance of eigenfrequencies, transformation of eigenmodes and we discuss the effect of boundary conditions and describe the transient example of Fig. 1. Final considerations conclude the paper.

## 2. Longitudinal waves in a rod

We start presenting the transformation of coordinates technique for a problem governed by a second-order differential equation. We show that for a rod the transformed equation maintains its form and the interface conditions are automatically satisfied eliminating any problem of reflection at the interface.

### 2.1. Equation of motion

We consider a thin rod having Young's modulus  $E$ , mass-density  $\rho$  and cross-sectional area  $A$ . The rod is shown in Fig. 2.

The longitudinal component  $U$  of the displacement vector  $\mathbf{U} = (U, V, W)$ , function of the position  $X$  and time  $t$ , satisfies the equation of motion (Graff, 1975)

$$[EA U_X(X, t)]_X = \rho A U_{tt}(X, t), \quad (1)$$

where subscripts indicate derivative with respect to the indicated variable, i.e.  $U_X = \partial U / \partial X$  and  $U_{tt} = \partial^2 U / \partial t^2$ . The axial force is  $N = EA U_X$ . For a homogeneous rod the longitudinal stiffness  $EA$  and the linear density  $\rho A$  are constant.

In the time-harmonic regime the displacement is  $\mathbf{U}(X, t) = \mathbf{U}(X)e^{-i\omega t}$ , with  $\omega$  the radian frequency, and the longitudinal component of the displacement satisfies the Helmholtz equation

$$[EA U_X(X)]_X + \rho A \omega^2 U(X) = 0. \quad (2)$$

### 2.2. Transformed equation

We introduce a coordinate transformation  $x = G(X)$ , with  $G(\cdot)$  injective function, and we indicate with  $g(x)$  the inverse function  $G^{-1}$ . First-order derivative in the original coordinate  $X$  and in the transformed one  $x$  are related by

$$\frac{d}{dX} = \frac{1}{g_x} \frac{d}{dx}. \quad (3)$$

Implementing the coordinate transformation in Eq. (2), we obtain the transformed equation of motion introducing a transformed displacement  $u(x)$  such that  $u(x) = U(X)$ . The transformed equation of motion has the form

$$[EA u_x(x)]_x + \bar{\rho} \bar{A} \omega^2 u(x) = 0, \quad (4)$$

which corresponds to an inhomogeneous rod having longitudinal stiffness  $\bar{E}\bar{A} = EA/g_x$  and linear density  $\bar{\rho}\bar{A} = g_x\rho A$ . In general, the transformed longitudinal stiffness and linear density are inhomogeneous. However, for affine transformations where  $g_x(x) = \text{const}$ , they reduce to the homogeneous case.

### 2.3. Interface boundary conditions

Let us apply the coordinate transformation in a domain  $X > X_0$ , where  $X_0$  is a given point. In such a case the problem is governed by the untransformed equation of motion (2) for  $X < X_0$  and by the transformed equation of motion (4) for  $X > X_0$ .

The untransformed and transformed domains have to share the same interface point, which means that the transformation has to satisfy the relation  $X_0 = g(x_0) = x_0$ . In addition, at the interface point  $X_0$  continuity conditions on the longitudinal displacement and on the axial force must be satisfied. We note that, if after transformation displacement  $u(x)$  or axial force  $n(x)$  change at the point  $X_0$ , a reflected wave will be generated. Clearly, zero reflection is required to have perfect match.

For the rod, in addition to the imposed equality  $u(x) = U(X)$ , we have

$$n(x) = \bar{E}\bar{A} \frac{d}{dx}[u(x)] = \frac{EA}{g_x} g_x \frac{d}{dX}[u(x)] = EA \frac{d}{dX}[U(X)] = N(X). \quad (5)$$

Therefore, both displacement  $u$  and axial force  $n$  in the transformed point  $x$  are equal to displacement  $U$  and axial force  $N$  in the original point  $X$ . These two equalities clearly hold also at the point  $X_0 = x_0$  assuring the absence of reflection at the interface.

### 2.4. Transformation for Perfectly Matched Layers in a rod

In addition to the perfect match, the transformation must damp the incoming waves; this target can be achieved by applying a complex transformation with  $g(x) = x + ih(x)$ , where the real function  $h(x) \geq 0$  and  $h(x_0) = 0$ . We note that, employing such a transformation, the generic wave  $\exp[ikX]$  is transformed into the wave  $\exp[k(-h(x) + ix)]$ , which decays exponentially fast. Such a model, based on coordinate transformation, include previously proposed PMLs obtained introducing artificial dissipation in the form of complex linear stiffness and density, respectively. In Sacks et al. (1995) complex material parameters were used to build PMLs for electromagnetic problems, which are governed by Helmholtz equations, while the conformal mapping technique was applied in Chang et al. (2014) in order to define PMLs for the plane elastodynamic problem governed by a system of second-order PDE. Here we consider the general transformation  $g(x) = x + i\alpha(x - x_0)^n$ , where  $\alpha$  and  $n$  are two parameters that can be varied in order to tune the wave damping. For the purpose of illustration, we show a comparison between an analytical solution and a numerical implementation for the infinite body Green's function. For the rod problem the time-harmonic Green's function expressing the displacement in  $X$  due to a unit force applied in  $X_c$  vibrates harmonically with frequency  $\omega$  is given by

$$U_g(X, X_c; \omega) = -\frac{1}{2k} \sin k|X - X_c|, \quad (6)$$

where  $k = \omega\sqrt{\rho/E}$  (see, for example, Graff (1975)).

In Fig. 3a we compare the analytical solution for the infinite body Green's function with a numerical solution with  $\alpha = 1$  and  $n = 1$ , implemented in *Comsol Multiphysics*® on a finite domain of total length of 20m and centered at  $X = 0$ . Two PML domains have been implemented in the boundary regions  $8\text{m} \leq |X| \leq 10\text{m}$  so that  $X_0 = \pm 8\text{m}$ , the radian frequency is  $\omega = \pi/2$ . Clamped boundary conditions are applied at  $X = \pm 10$ , they are known to generate larger amplitude reflected waves with respect to other type of

boundary conditions (Jones et al., 2015). We stress the excellent agreement between the analytical and numerical solutions and the wave damping within the PML regions. The agreement between the analytical and numerical solutions demonstrates the matching at the interface points  $X_0 = \pm 8$  and the absence of reflection. In part (b) we compare two numerical solutions obtained applying an affine transformation with  $\alpha = 1$ ,  $n = 1$  and a non-affine transformation with  $\alpha = 3$ ,  $n = 4$ . The results, given for  $\omega = \pi$  and reported only in the region  $X \geq 0$ , show again excellent agreement in the central region and the increased damping for the second choice of material parameters.

In conclusion of this Section we note that the transformation is frequency independent and, therefore, the PMLs work equally well at different frequencies subjected to the usual limitations on the mesh size with respect to the wavelength.

## 3. Flexural waves in a beam

In this Section we apply the transformation coordinates technique for flexural waves in a slender beam, governed by a fourth-order differential equation. We give a physical interpretation of the transformed equations as in Brun et al. (2014a) and Colquitt et al. (2014). We also show that, under coordinate transformation, the transformed medium possesses the same eigenfrequencies as the original one, a property that can be used in order to check to correctness of the transformation in finite domains with evident advantages on the implementation.

### 3.1. Equation of motion

We consider time-harmonic transverse displacements  $V(X, t) = V(X)e^{-i\omega t}$  in a slender beam structure as in Fig. 2. The beam has cross-sectional area  $A$ , second-moment of inertia  $J$ , Young's modulus  $E$  and density  $\rho$ . The equation of motion for  $V(x)$  is

$$[EJV_{xx}(X)]_{xx} - \rho A \omega^2 V(X) = -T_X(X) - \rho A \omega^2 V(X) = 0. \quad (7)$$

where  $T(X) = M_X(X) = -[EJV_{xx}(X)]_X$  is the shear force and  $M(X)$  the bending moment. The transverse displacement component  $W(X)$  is governed by an analogous fourth-order differential equation.

### 3.2. Transformed equation

Again, we introduce the transformation  $x = G(X)$ , with inverse transformation  $X = g(x)$ . Then, the transformed equation has the form

$$[t(x) + n(x)v_x(x)]_x + \bar{\rho}\bar{A}(x)\omega^2 v(x) = 0, \quad (8)$$

where  $v(x)$  is the transformed transverse displacement, that we assume equal to  $V(X)$ . The transformed shear and axial forces are given by

$$\begin{aligned} t(x) &= m_x(x) = -[EJ(x)v_{xx}(x)]_x, \\ n(x) &= \frac{3g_{xx}^2(x) - g_{xxx}(x)g_x(x)}{g_x^5(x)} EJ, \end{aligned} \quad (9)$$

respectively, where  $m(x)$  is the transformed bending moment. The bending stiffness and linear density transform as follows

$$\bar{E}J(x) = \frac{EJ}{g_x^3}, \quad \bar{\rho}\bar{A}(x) = g_x\rho A. \quad (10)$$

We note that the equation of motion (8) represents an inhomogeneous beam in presence of axial stress (see Brun et al. (2014b); Colquitt et al. (2014)).

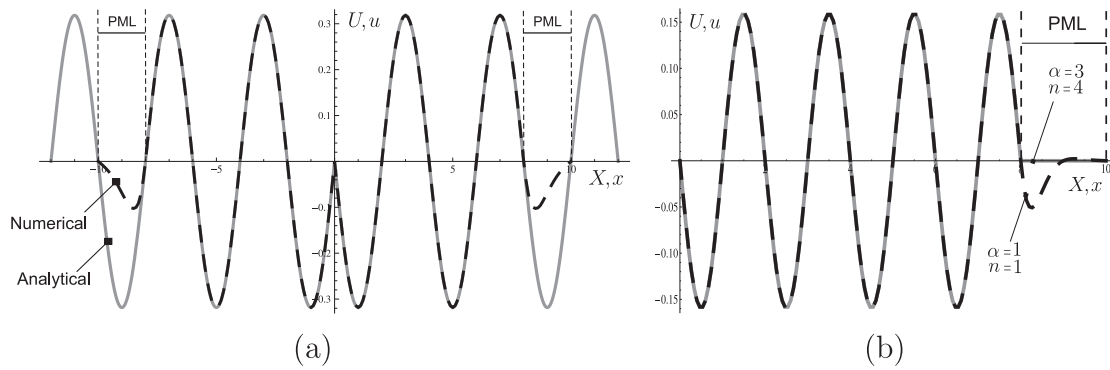


**Fig. 3.** Time-harmonic infinite body Green's function in rod structures. Results are given for  $k = 1 \text{ m}^{-1}$ . (a) Comparison between analytical solution (6) for an infinite rod and numerical solution implemented in *Comsol Multiphysics*® for a finite system, with  $|X| \leq 10\text{m}$  and radian frequency  $\omega = \pi/2$ . The PMLs have been implemented employing a transformation with  $\alpha = 1$  and  $n = 1$ . (b) Comparison between numerical solutions with transformation parameters  $\alpha = 1$ ,  $n = 1$  and  $\alpha = 3$ ,  $n = 4$ . Results are given for  $\omega = \pi$  and are shown only in the region  $0 \leq X \leq 10\text{m}$ .

### 3.3. Interface conditions

At the interface  $X_0 = x_0$  between untransformed and transformed domains the following essential conditions

$$\begin{cases} V(X_0) = v(x_0), \\ V_X(X_0) = v_X(x_0), \end{cases} \quad (11)$$

and natural conditions

$$\begin{cases} M(X_0) = m(x_0), \\ T(X_0) = t(x_0) + n(x_0)v_X(x_0), \end{cases} \quad (12)$$

must be satisfied.

Expressing the interface conditions in the transformed domain as a function of the original variable  $X$ , of the original displacement  $V(X)$  and of the inverse transformation function  $g(x)$ , we obtain after simple algebraic manipulations

$$\begin{cases} v(x_0) = V(X_0), \\ v_X(x_0) = g_X(x_0)V_X(X_0), \\ m(x_0) = -EJ \frac{g_X^2(x_0)V_{XX}(X_0) + g_{XX}(x_0)V_X(X_0)}{g_X^3(x_0)}, \\ r(x_0) = t(x_0) + n(x_0)v_X(x_0) = EJ \frac{3g_X^2(x_0) - g_{XXX}(x_0)g_X(x_0)}{g_X^4(x_0)} V(X_0) \\ \quad - EJ \frac{g_X^3(x_0)V_{XXX}(X_0) + 3g_X(x_0)g_{XX}(x_0)V_{XX}(X_0) + g_{XXX}(x_0)V_X(X_0)}{g_X^3(x_0)}. \end{cases} \quad (13)$$

Then, the constraints

$$g_X(x_0) = 1, \quad g_{XX}(x_0) = 0, \quad g_{XXX}(x_0) = 0, \quad (14)$$

in Eq. (13) assure that interface conditions (11) and (12) are satisfied independently on the general choice of the transformation  $G(X)$  or of its inverse  $g(x)$ . The three conditions in Eq. (14) must be complemented by the additional condition  $X_0 = g(x_0) = x_0$ , which identifies the same interface point between untransformed and transformed domains.

We note that transformed bending stiffness and linear density, defined in Eq. (9), are homogeneous only for affine transformation. However, the only admissible affine transformation for the beam case is the identity in view of the constraints  $g(x_0) = X_0$  and  $g_X(x_0) = 1$ , which means that an inhomogeneous material is needed in the transformed domain.

### 3.4. Eigenfrequency analysis

Here we compare eigenfrequencies and eigenmodes for a homogeneous beam defined in the domain  $-L \leq X \leq L$  and for a second beam structure where we apply a transformation on the right

half of the structure  $0 \leq X \leq L$  which transforms into the domain  $0 \leq x \leq l$ , as shown in Fig. 4a. We consider a polynomial transformation  $g(x)$  subjected to the constraints as in Eq. (14) and  $x_0 = g(x_0) = X_0$  at the interface point  $x_0 = X_0 = 0$ . In addition, we impose  $g(l) = L$ , which defines the length of the transformed domain and the additional conditions

$$g_X(l) = 1, \quad g_{XX}(l) = 0, \quad g_{XXX}(l) = 0, \quad (15)$$

assuring, in view of relations (13), the direct identification of the same boundary conditions on rotation, moment and vertical force at the boundary point  $x = l$ , as demonstrated in the previous Section. The corresponding transformation is the monotonically increasing septic polynomial

$$g(x) = x + 35 \frac{L-l}{l^4} x^4 - 84 \frac{L-l}{l^5} x^5 + 70 \frac{L-l}{l^6} x^6 - 20 \frac{L-l}{l^7} x^7. \quad (16)$$

Coordinate transformation (16) does not depend on the boundary conditions. For specific boundary conditions it is not necessary to impose all conditions (15); for example, in the case of a simple support, where  $V(L) = 0$ ,  $V_{XX}(L) = 0$ ,  $V_X(L) \neq 0$  and  $V_{XXX}(L) \neq 0$ , only the conditions  $g_X(l) = 1$ ,  $g_{XX}(l) = 0$  are needed to assure that the bending moment  $m(l)$  is zero in addition to the displacement  $v(l)$  (see Eq. (13)). Nevertheless, we have proposed transformation (15) which includes all possible boundary conditions.

We also note that, apart from satisfaction of conditions at interface and boundary points, there is complete freedom in the choice of the transformation  $g(x)$  within a properly defined set of functions.

Restricting the attention to a simply supported beam, the homogeneous problem governed by the Eq. (7) has solution

$$V(X) = A_1 e^{i\beta X} + A_2 e^{-\beta X} + A_3 e^{-i\beta X} + A_4 e^{\beta X}, \quad (17)$$

where  $\beta^4 = (\rho A)/(EJ)\omega^2$ ; such a solution, supplemented by the boundary conditions  $V(-L) = V(L) = 0$ ,  $V_{XX}(-L) = V_{XX}(L) = 0$ , gives the well known result that eigenfrequencies are  $\omega = (p\pi)^2/(4L^2)\sqrt{(EJ)/(\rho A)}$  ( $p$  positive integer number) and the corresponding eigenmodes are  $V(X) = \sin[p\pi(X+L)/(2L)]$ .

For the problem in which the region  $0 \leq X \leq L$  has been transformed into the region  $0 \leq x \leq l$  by mean of the transformation (16), the solution (17) is still valid within the domain  $-L \leq X \leq 0$ , while in the domain  $0 \leq x \leq l$  the problem is governed by the transformed equation of motion, given in Eq. (8). In such a domain the inhomogeneous bending stiffness and linear density are

$$\begin{aligned} \bar{EJ} &= \frac{EJ}{\left(1 + 140 \frac{L-l}{l^4} x^3 - 420 \frac{L-l}{l^5} x^4 + 420 \frac{L-l}{l^6} x^5 - 140 \frac{L-l}{l^7} x^6\right)^3}, \\ \bar{\rho A} &= \left(1 + 140 \frac{L-l}{l^4} x^3 - 420 \frac{L-l}{l^5} x^4 + 420 \frac{L-l}{l^6} x^5 - 140 \frac{L-l}{l^7} x^6\right) \rho A, \end{aligned} \quad (18)$$

respectively.



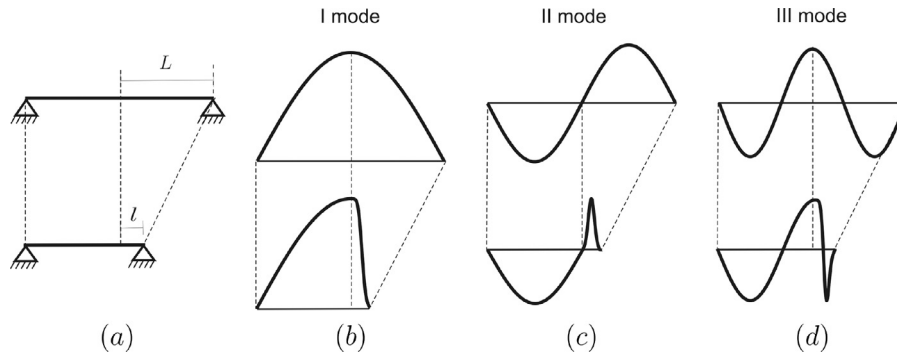


**Fig. 4.** Eigenmodes of homogeneous beam of length  $2L$  and inhomogeneous beam of length  $L + l$ . (a) Simply supported beams: the inhomogeneous beam has been obtained from transformation (16), the half-length  $L = 1$  m is transformed into the length  $l = 0.2$  m. (b) First eigenmodes for the two structures at  $\omega = \pi^2/(4L^2)\sqrt{(EJ)/(\rho A)}$ . (c) Second eigenmodes at  $\omega = 4\pi^2/(4L^2)\sqrt{(EJ)/(\rho A)}$ . (d) Third eigenmodes at  $\omega = 9\pi^2/(4L^2)\sqrt{(EJ)/(\rho A)}$ .

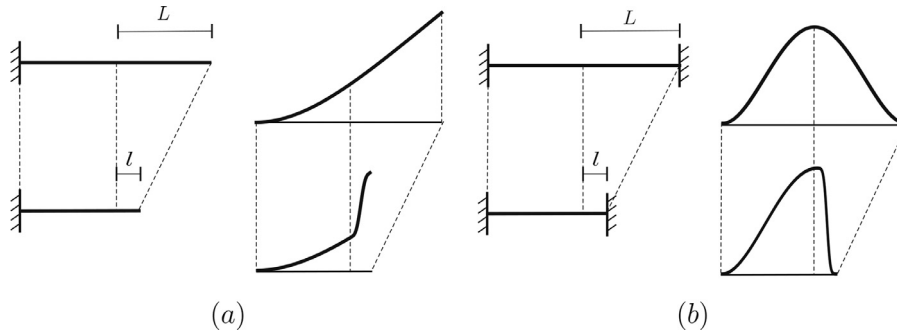


**Fig. 5.** Eigenmodes of homogeneous beam of length  $2L$  and inhomogeneous beam of length  $L + l$ ,  $L = 1$  m and  $l = 0.2$  m. (a) Clamped-free boundary conditions: the first eigenmode is shown, the eigenfrequency is  $\omega = (0.597\pi)^2/(4L^2)\sqrt{(EJ)/(\rho A)}$ . (b) Clamped-clamped boundary conditions: the first eigenmode is shown, the eigenfrequency is  $\omega = (1.505\pi)^2/(4L^2)\sqrt{(EJ)/(\rho A)}$ .

The equation of motion for the transformed domain has the general solution

$$v(x) = B_1 e^{i\beta g(x)} + B_2 e^{-\beta g(x)} + B_3 e^{-i\beta g(x)} + B_4 e^{\beta g(x)}, \quad (19)$$

The system of two equations of motion is supplemented by the four boundary conditions  $V(-L) = v(l) = 0$ ,  $V_{xx}(-L) = v_{xx}(l) = 0$  and by the four interface conditions given in Eqs. (11) and (12), where  $X_0 = x_0 = 0$ .

Eigenfrequencies and eigenmodes are obtained from the eigenvalues and eigenvectors of the system of equations  $\mathbf{M}\mathbf{a} = \mathbf{0}$  given by the 8 boundary and interface conditions, where  $\mathbf{a} = [A_1 A_2 A_3 A_4 B_1 B_2 B_3 B_4]^T$  is the vector of the unknown amplitudes and the matrix  $\mathbf{M}$  collects the coefficients of the equations. Then, the condition

$$\det \mathbf{M} = 256(EJ)^2 \beta^{10} \sin(2\beta L) \sinh(2\beta l) = 0, \quad (20)$$

gives exactly the same eigenfrequencies of the homogeneous system, namely  $\omega = (p\pi)^2/(4L^2)\sqrt{(EJ)/(\rho A)}$  ( $p$  positive integer) and the trivial one  $\omega = 0$ . The first 3 eigenmodes for the homogeneous and not homogeneous systems are given in Fig. 4b–d. In particular, we note that the solution in the transformed domain is  $v(x) = V[g(x)] = V(X)$ .

In Fig. 5 we report the first eigenmode for the two structures for different boundary conditions and the same transformation given in Eq. (16): clamped-free in part (a) and clamped-clamped in part (b). Again, the eigenfrequencies for the homogeneous and inhomogeneous systems coincide and the eigenmodes in the transformed domain are such that  $v(x) = V(X)$ .

We note that, while the coincidence of eigenfrequencies can be expected, it depends on the boundary conditions which, in the case of flexural waves, are not preserved by a general transformation, as shown previously. We also stress that, to the best of our

knowledge, such a comparison has never been considered before to check the connection between the solutions before and after transformation.

### 3.5. Perfectly Matched Layers in a beam

In order to define the Perfectly Matched Layer we consider a complex transformation such that  $g(x) = g^R(x) + ig^I(x)$ , where  $g^R(x)$  and  $g^I(x)$  stand for the real and imaginary parts. The constraints of Eq. (14) at the interface point  $X_0 = x_0$  plus the condition  $g(x_0) = x_0$  imply that

$$\begin{cases} g^R(x_0) = x_0, & g^I(x_0) = 0, \\ g_x^R(x_0) = 1, & g_x^I(x_0) = 0, \\ g_{xx}^R(x_0) = g_{xx}^I(x_0) = 0, \\ g_{xxx}^R(x_0) = g_{xxx}^I(x_0) = 0. \end{cases} \quad (21)$$

Therefore, if we consider a polynomial transformation, the real and imaginary parts  $g^R(x)$  and  $g^I(x)$ , respectively, must be at least polynomials of degree 4 in  $(x - x_0)$  and, for the imaginary part, the lowest non-zero term has at least power 4.

### 3.6. Additional boundary condition

In the implementation of the Perfectly Matched Layer within a Finite Element code the infinite domain is substituted by a finite domain, which introduces an additional boundary condition at the boundary  $x = x_1$  of the Perfectly Matched Layer domain. In general, this boundary condition perturbs the infinite domain solution.

By looking at the solution (19) of the transformed problem, we note that the propagating solution  $B_1 e^{i\beta g(x)} + B_2 e^{-\beta g(x)}$  is generated at the interface at  $x = x_0$ , while the reflected solution

$B_3 e^{-i\beta g(x)} + B_4 e^{\beta g(x)}$  is generated at the fictitious boundary  $x = x_1$ . Therefore, a possible approach in order to eliminate the perturbation introduced by the additional boundary conditions, is to define ad-hoc boundary conditions at  $x = x_1$  that would eliminate the reflected solution, namely boundary conditions leading to  $B_3 = B_4 = 0$ . The fields at  $x = x_1$  can be written in the partitioned form

$$\begin{bmatrix} \mathbf{A}_{11} & \mathbf{A}_{12} \\ \mathbf{A}_{21} & \mathbf{A}_{22} \end{bmatrix} \begin{pmatrix} \mathbf{b}_1 \\ \mathbf{b}_2 \end{pmatrix} = \begin{pmatrix} \mathbf{c}_1 \\ \mathbf{c}_2 \end{pmatrix} \quad (22)$$

where

$$\mathbf{b}_1 = \begin{pmatrix} B_1 \\ B_2 \end{pmatrix}, \quad \mathbf{b}_2 = \begin{pmatrix} B_3 \\ B_4 \end{pmatrix},$$

$$\mathbf{c}_1 = \begin{pmatrix} v(x_1) \\ v_x(x_1) \end{pmatrix}, \quad \mathbf{c}_2 = \begin{pmatrix} m(x_1) \\ r(x_1) \end{pmatrix}, \quad (23)$$

and

$$\mathbf{A}_{11} = \begin{bmatrix} e^{i\beta g(x_1)} & e^{-\beta g(x_1)} \\ i\beta g_x(x_1) e^{i\beta g(x_1)} & -\beta g_x(x_1) e^{-\beta g(x_1)} \end{bmatrix},$$

$$\mathbf{A}_{12} = \begin{bmatrix} e^{-i\beta g(x_1)} & e^{\beta g(x_1)} \\ -i\beta g_x(x_1) e^{-i\beta g(x_1)} & \beta g_x(x_1) e^{\beta g(x_1)} \end{bmatrix},$$

$$\mathbf{A}_{21} = EJ\beta \begin{bmatrix} \frac{e^{i\beta g(x_1)} [\beta g_x^2(x_1) - i g_{xx}(x_1)]}{g_x^3(x_1)} & -\frac{e^{-\beta g(x_1)} [\beta g_x^2(x_1) - g_{xx}(x_1)]}{g_x^3(x_1)} \\ \frac{i e^{i\beta g(x_1)} \eta_1(x)}{g_x^4(x_1)} & \frac{e^{-\beta g(x_1)} \eta_2(x)}{g_x^4(x_1)} \end{bmatrix},$$

$$\mathbf{A}_{22} = EJ\beta \begin{bmatrix} \frac{e^{-i\beta g(x_1)} [\beta g_x^2(x_1) + i g_{xx}(x_1)]}{g_x^3(x_1)} & -\frac{e^{\beta g(x_1)} [\beta g_x^2(x_1) + g_{xx}(x_1)]}{g_x^3(x_1)} \\ -\frac{i e^{-i\beta g(x_1)} \eta_1(x)}{g_x^4(x_1)} & -\frac{e^{\beta g(x_1)} \eta_2(x)}{g_x^4(x_1)} \end{bmatrix}, \quad (24)$$

with

$$\eta_1(x) = \beta^2 g_x^4(x_1) + 6g_{xx}(x_1)^2 - 2g_x(x_1)g_{xxx}(x_1),$$

$$\eta_2(x) = \beta^2 g_x^4(x_1) - 6g_{xx}(x_1)^2 + 2g_x(x_1)g_{xxx}(x_1). \quad (25)$$

If we substitute the solution  $\mathbf{b}_1 = \mathbf{A}_{11}^{-1}[\mathbf{c}_1 - \mathbf{A}_{12}\mathbf{b}_2]$  of the first pair of equations in (23), into the second pair of equations, we obtain

$$(\mathbf{A}_{22} - \mathbf{A}_{21}\mathbf{A}_{11}^{-1}\mathbf{A}_{12})\mathbf{b}_2 = \mathbf{c}_2 - \mathbf{A}_{21}\mathbf{A}_{11}^{-1}\mathbf{c}_1. \quad (26)$$

The solution of the system of two equations (26) is zero, i.e.  $B_3 = B_4 = 0$ , if

$$\mathbf{c}_2 = \mathbf{A}_{21}\mathbf{A}_{11}^{-1}\mathbf{c}_1, \quad (27)$$

provided that

$$\det[\mathbf{A}_{22} - \mathbf{A}_{21}\mathbf{A}_{11}^{-1}\mathbf{A}_{12}] \neq 0 \text{ and } \det[\mathbf{A}_{11}] \neq 0. \quad (28)$$

The two conditions in (27) express the natural boundary conditions  $m(x_1)$  and  $r(x_1)$  as a function of the essential boundary conditions  $v(x_1)$  and  $v_x(x_1)$ . The explicit expressions are

$$m(x_1) = EJ \frac{-i\beta^2 g_x^3(x_1)v(x_1) + [-g_{xx}(x_1) + (1-i)\beta g_x^2(x_1)]v_x(x_1)}{g_x^4(x_1)},$$

$$r(x_1) = EJ \frac{(1+i)\beta^3 g_x^5(x_1)v(x_1) + [\eta_1(x_1) + (i-1)\beta^2 g_x^4(x_1)]v_x(x_1)}{g_x^5(x_1)}, \quad (29)$$

where  $\eta_1$  is given in Eq. (25). We note that the two determinants in Eq. (28) can be always set different from zero for every  $\beta$  by modulating the quantity  $g(x_1)$ .

The Perfectly Matched Layer and the optimal boundary conditions given in Eq. (29) have been implemented in the Finite Element code *Comsol Multiphysics*<sup>®</sup>. In particular, we consider the infinite body time-harmonic Green's function, which has the analytical expression

$$V_g(X, X_c; \omega) = \frac{1}{4EJ\beta^3} [e^{-\beta|X-X_c|} + \sin(\beta|X-X_c|)], \quad (30)$$

as in Brun et al. (2012). The analytical expression is compared with numerical simulations. We considered the following structural parameters:  $EJ = 1$  MPa,  $\rho A = 1$  kg/m,  $X_c = 0$  m,  $X_0 = x_0 = 8$  m and  $x_1 = 10$  m. The implemented inverse transformation is

$$g(x) = x \mp \frac{35(x_1 - 2x_0)}{(x_1 - x_0)^4} (x \mp x_0)^4 + \frac{84(x_1 - 2x_0)}{(x_1 - x_0)^5} (x \mp x_0)^5$$

$$\mp \frac{70(x_1 - 2x_0)}{(x_1 - x_0)^6} (x \mp x_0)^6 + \frac{20(x_1 - 2x_0)}{(x_1 - x_0)^7} (x \mp x_0)^7$$

$$+ i(x \mp x_0)^\alpha, \quad (31)$$

where  $\mp$  stands for the PML domains at  $x \in (\pm x_0, \pm x_1)$  and  $\alpha = 5$ . Transformation (31) has been obtained applying conditions (21), where  $x_0$  stands for  $\pm x_0$  and conditions

$$g^R(\pm x_1) = \pm 2x_0, \quad g_x^R(\pm x_1) = 1, \quad g_{xx}^R(\pm x_1) = 0, \quad g_{xxx}^R(\pm x_1) = 0 \quad (32)$$

on the real part of the transformation. Additional conditions on the imaginary part of the transformation  $g^I$  at  $x = \pm x_1$  have not been applied since they lead to larger amplitude reflected fields.

The deformed shapes are given in gray lines in Fig. 6a for different discretizations, while the dashed black line indicates the analytical solution as in Eq. (30). The comparative analysis shows that the results converge towards the analytical solution in the central region increasing the number of elements. In the PML regions it is evident the damping of the wave.

We define the *quality factor*, the measure

$$\mathcal{Q} = \int_{-X_0}^{+X_0} \left( \frac{V(X) - V_g(X, 0; \omega)}{V_g(0, 0; \omega)} \right)^2 dX, \quad (33)$$

where  $V(X)$  is the solution in the untransformed domain  $X \in (-X_0, X_0)$ .  $\mathcal{Q}$  is a quantitative description of the quality of the PML, which tends to 0 for perfect PMLs, indicating the absence of perturbation within the central domain  $X \in (-X_0, X_0)$ . In Fig. 6b the *quality factor*  $\mathcal{Q}$  is shown as a function of the size  $s$  of the elements in double logarithmic scale. For simplicity, in each computation we considered elements of the same size  $s$ . The results show an excellent convergence of the numerical results toward the analytical solution. The linear regression, indicated with a dashed line in Fig. 6b, indicates that the quality factor  $\mathcal{Q}$  goes to zero as  $6.78s^{8.14}$ .

### 3.7. Perfectly Matched Layers with standard boundary conditions

In Section 3.6 we detailed how to implement perfect PMLs proposing an optimal solution for the additional boundary conditions introduced in the finite domain implemented numerically. Such a model gives excellent results, but has two limitations: first, it is difficult to implement in a standard Finite Element code and second, boundary conditions are frequency dependent. Specifically, relations (29) between different boundary conditions depend on the parameter  $\beta \propto \sqrt{\omega}$  and the frequency dependence limits the applicability of the proposed model to transient problems.

Here, we propose a simpler solution with frequency independent boundary conditions. In particular, we implement classical boundary conditions at  $x = \pm x_1$ , namely clamped, free and simply supported.

When these classical boundary conditions are implemented in *Comsol Multiphysics*<sup>®</sup> the obtained displacement fields, not reported here for brevity, show again an excellent agreement with the analytical results in the central region. In Fig. 7 we report the *quality factor*  $\mathcal{Q}$  as a function of the normalized frequency  $m_0\beta = (x_1 - x_0)\beta$  for  $\alpha = 4$  in Eq. (31). The *quality factor*  $\mathcal{Q}$  has been computed from the analytical solutions for the infinite medium and the finite medium with PMLs in order to check the effect of the boundary conditions independently on the influence of the discretization.

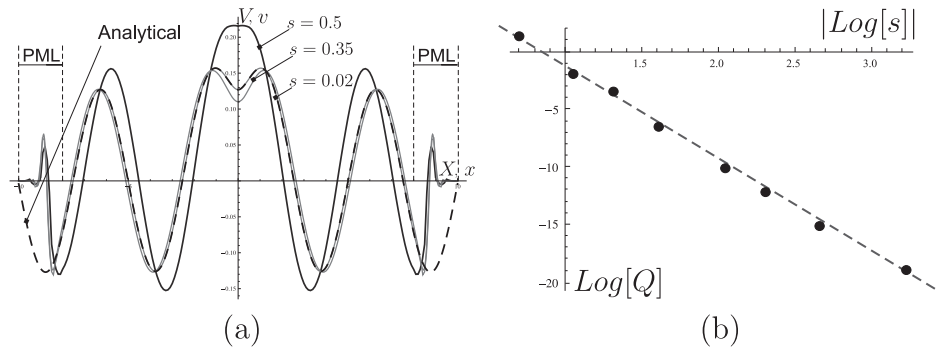


**Fig. 6.** Fig (a) Time-harmonic Green's function. The analytical displacement of Eq. (30) is given in black dashed line. The numerical results are given in continuous gray lines. Different curves correspond to different size  $s$  of the elements given in meter; the elements have constant length within the domain  $(-x_1, x_1) = (-10\text{m}, 10\text{m})$  (b) Quality factor  $Q$  as a function of the size  $s$  of the element. Results are given in logarithmic scale.

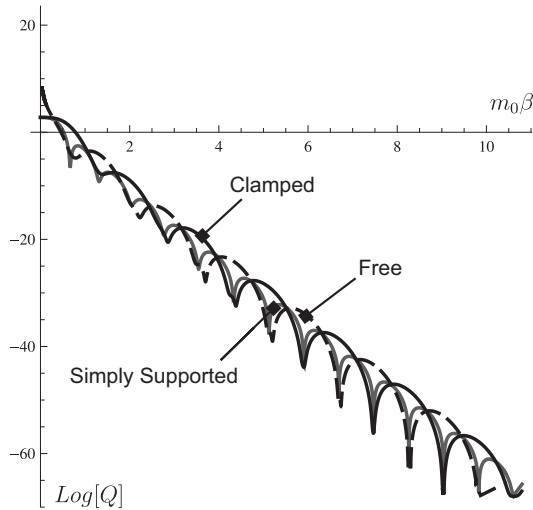


**Fig. 7.** Quality factor  $Q$  as a function of the normalized frequency  $m_0\beta$ . Results are given for the same mechanical parameters of Fig. 6. Continuous black line corresponds to simply supported boundary conditions, continuous gray line to free boundaries and dashed black line to clamped boundaries.

The convergence increases with frequency and the three boundary conditions give equivalent results with a preference on the simply supported case at the lowest frequencies. Increasing the exponent  $\alpha$  in the imaginary part of  $g(x)$  in Eq. (31) gives equivalent results with the difference that the number of asymptotes in the quality factor  $Q$  curves as a function of  $\beta$  increases with  $\alpha$ .

### 3.8. Dimension of the layer

In order to estimate the error introduced by the layer of dimension  $m_0 = |x_1 - x_0|$ , we consider an incident plane wave  $w_I(X) = e^{i\beta X}$  impinging the interface between the homogeneous domain and the PML at  $X_0 = x_0 = 0$  and generating the reflected wave  $w_R(X) = R_1 e^{-i\beta X} + R_2 e^{\beta X}$  and the transmitted wave  $w_T(x) = T_1 e^{i\beta g(x)} + T_2 e^{-\beta g(x)} + T_3 e^{-i\beta g(x)} + T_4 e^{\beta g(x)}$ , where the six constants  $R_1, R_2, T_1, T_2, T_3, T_4$  can be easily found by imposing the four interface conditions at  $x = x_0 = 0$  and two boundary conditions at  $x = x_1 = x_0 + m_0$ . The solution, for different boundary conditions has the form  $T_1 = 1, T_2 = 0$ , indicating the perfect match at the interface, and  $R_1 = T_3, R_2 = T_4$ , showing that the reflected wave is generated by the boundary conditions at  $x = x_1$ . In particular, for perfect boundary conditions as in Eq. (29) there is no reflection, i.e.  $R_1 = T_3 = R_2 = T_4 = 0$  and, in principle, the only boundary conditions (29) are sufficient to avoid reflection without the need to introduce a PML. For clamped, simply supported and free bound-

ary conditions the reflected amplitudes are

$$|R_1| = f_1(m_0, \beta) e^{-2m_0^\alpha \beta}, \quad |R_2| = f_2(m_0, \beta) e^{-m_0^\alpha \beta}, \quad (34)$$

where  $f_1(m_0, \beta)$  and  $f_2(m_0, \beta)$  are  $\mathcal{O}(1)$  in  $m_0$  and  $\beta$  and  $\alpha$  is the exponent of the imaginary part of the transformation (31). For all boundary conditions, including the perfect ones, the displacement amplitude decays exponentially as  $e^{-m_0^\alpha}$ , while (Nataf, 2013) indicates that for problems governed by Helmholtz equations the reflection coefficients decay exponentially as  $e^{-2m_0}$ . Results consistent with Nataf (2013) are obtained if null conditions are applied at  $\pm x_1$  to  $g^I$  and to its first three derivatives.

### 3.9. Transient load results

The PMLs with simply supported boundary conditions has been tested for a transient load as given in Fig. 1. For the transient regime the following equations of motion have been solved numerically:

$$[E]V_{xx}(X, t)_{XX} + \rho A V_{tt}(X, t) = 0 \quad (35)$$

in the untransformed domain  $D_1$  and

$$[(\bar{E}J(x)v_{xx}(x, t))_x - n(x)v_x(x, t)]_x + \bar{\rho}\bar{A}(x)v_{tt}(x, t) = 0, \quad (36)$$

in the transformed one  $D_2$ , where  $\bar{E}J(x)$  and  $\bar{\rho}\bar{A}(x)$  are given in Eq. (10) and  $n(x)$  is given in Eq. (9) and they are the same as in the time-harmonic regime. Zero initial boundary conditions have been applied, namely

$$V(X, 0) = v(x, 0) = 0, \quad V_t(X, 0) = v_t(x, 0) = 0, \quad X \in D_1, \quad x \in D_2. \quad (37)$$

The time variation of the point load

$$F(t) = \sum_{i=1}^6 [(-1)^{i+1} 10i e^{1000(t-0.08i)^2}] \quad (38)$$

is shown in Fig. 8 and it has been applied at  $X = 0$ . Two geometries have been implemented in Finite Elements: a larger one with homogeneous properties  $EJ = 1 \text{ Pa}$ ,  $\rho A = 1 \text{ kg/m}$  and  $X \in [-20\text{m}, 20\text{m}]$  and a shorter one with the same homogeneous properties in  $X \in [-4\text{m}, 4\text{m}]$  and PMLs in  $|X| \in [4\text{m}, 7\text{m}]$ . The transformation is given in Eq. (31) with  $\alpha = 5$  and it is unchanged with respect to the time-harmonic regime since it involves only a spatial transformation.

The two initial boundary value problems have been solved in Comsol using a backward differentiation formula; a total period of 5 s has been analyzed and standard convergence analysis has been considered on the time steps and element size; the initial step has been set to  $10^{-4}$  s and elements of uniform size  $s = 5 \text{ cm}$  have been implemented.

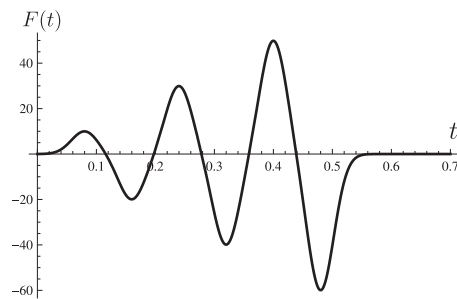


Fig. 8. Time distribution of the point load applied at  $X = 0$  in the transient analysis.

The transverse displacement is given in Fig. 1 at  $t = 0.5$  s, when the propagating wave has reached the fictitious boundary at  $x_1 = \pm 7$  m but not the boundaries  $X = \pm 20$  m for the larger domain. In the Figure only the region  $X \in [-10 \text{ m}, 10 \text{ m}]$  is shown for visualization purposes. The comparison between the two numerical solutions evidences an excellent agreement in the central region where PMLs are not present. Such an example reveals the competitive behavior of the proposed technique in the transient regime; this is expected since only a spatial transformation  $g(x)$  is implemented. Nevertheless, a complete analysis of the transient response requires a different type of study which is left for a future work.

#### 4. Conclusions

We have proposed an analytical PML model for flexural waves. The excellent agreement with analytical Green's function for infinite domain is detailed, the error in the case of non-perfect additional boundary conditions is estimated and the influence of discretization is also given.

We have given particular importance to the physical interpretation of the transformed equations in order to show that the method is simple and can be implemented in standard finite element packages; the eigenfrequency analysis may also be used as a simple check of the correctness of the implementation.

The PMLs for flexural waves can be particularly useful in the analysis of elongated structures like bridges and pipelines and comparisons with analytical results for infinitely long structures (Carta et al., 2014; Carta and Brun, 2015).

#### References

- Aliabadi, M., 2002. *The Boundary Element Method, Applications in Solids and Structures*, 2. John Wiley Andamp, Sons, Ltd, West Sussex, England.
- Astley, R., Hamilton, J., 2006. The stability of infinite elements schemes for transient wave problems. *Comput. Methods Appl. Mech. Eng.* 195 (29–32), 3553–3571. doi:10.1016/j.cma.2005.01.026.
- Beer, G., 2001. *Programming the Boundary Element Method: An Introduction for Engineers*, 1. Wiley, Chichester, England.
- Berenger, J., 1994. A perfectly matched layer for the absorption of electromagnetic waves. *J. Comput. Phys.* 114 (2), 185–200. doi:10.1006/jcph.1994.1159.
- Bertoldi, K., Brun, M., Bigoni, D., 2005. A new boundary element technique without domain integrals for elastoplastic solids. *Int. J. Numer. Methods Eng.* 64, 877–906. doi:10.1002/nme.1385.
- Bettess, P., 1992. *Infinite Elements*. Penhshaw Press, U.K.
- Bettess, P., Zienkiewicz, O., 1977. Diffraction and refraction of surface waves using finite and infinite elements. *Int. J. Numer. Methods Eng.* 11 (8), 1271–1290. doi:10.1002/nme.1620110808.
- Bonnet, M., 1999. *Boundary Integral Equation Methods for Solids and Fluids*. Wiley, Chichester.
- Brun, M., Bigoni, D., Capuani, D., 2003. A boundary element technique for incremental, non-linear elasticity. part ii: bifurcation and shear bands. *Comput. Methods Appl. Mech. Eng.* 192, 2481–2499. doi:10.1016/S0045-7825(03)00272-X.
- Brun, M., Capuani, D., Bigoni, D., 2003. A boundary element technique for incremental, non-linear elasticity. part i: formulation. *Comput. Methods Appl. Mech. Eng.* 192, 2461–2479. doi:10.1016/S0045-7825(03)00268-8.
- Brun, M., Colquitt, D., Jones, I., Movchan, A., Movchan, N., 2014. Transformation cloaking and radial approximations for flexural waves in elastic plates. *New J. Phys.* 16, 093020. doi:10.1088/1367-2630/16/9/093020.

- Brun, M., Colquitt, D., Jones, I., Movchan, A., Movchan, N., 2014. Transformation cloaking and radial approximations for flexural waves in elastic plates. *New J. Phys.* 16. doi:10.1088/1367-2630/16/9/093020.
- Brun, M., Giaccu, G., Movchan, A.B., Movchan, N., 2012. Asymptotics of eigenfrequencies in the dynamic response of elongated multi-structures. *Proc. R. Soc. Lond. A* 468 (2138), 378–394. doi:10.1098/rspa.2011.0415.
- Brun, M., Guenneau, S., Movchan, A., 2009. Achieving control of in-plane elastic waves. *Appl. Phys. Lett.* 94, 061903. doi:10.1063/1.3068491.
- Burnett, D., 1994. A three-dimensional acoustic infinite element based on a generalized multipole expansion. *J. Acoust. Soc. Am.* 96 (5), 2798–2816. doi:10.1121/1.411286.
- Carta, G., Brun, M., 2015. Bloch-floquet waves in flexural systems with continuous and discrete elements. *Mech. Mater.* 87, 11–26. doi:10.1016/j.mechmat.2015.03.004.
- Carta, G., Brun, M., Movchan, A., 2014. Dynamic response and localization in strongly damaged waveguides. *Proc. R. Soc. A. Math. Phys. Eng. Sci.* 470 (20140136). doi:10.1098/rspa.2014.0136.
- Cerjan, C., Kosloff, D., Kosloff, R., Reshef, M., 1985. Absorbing boundary conditions for the numerical simulation of waves. *Geophysics* 50, 705–708. doi:10.1190/1.1441945.
- Chang, Z., Guo, D., Feng, X., Hu, G., 2014. A facile method to realize perfectly matched layers for elastic waves. *Wave Motion* 51 (7), 1170–1178. doi:10.1016/j.wavemoti.2014.07.003.
- Chew, W., Weedon, W., 1994. A 3d perfectly matched medium modified maxwell's equations with stretched coordinates. *Microwave Optical Tech. Lett.* 7 (13), 599–604. doi:10.1002/mop.4650071304.
- Clouteau, D., Cotteneau, R., Lombaert, G., 2000. A review on the modelling of wheel/rail noise generation. *J. Sound Vib.* 231 (3), 519–536. doi:10.1006/jsvi.1999.2542.
- Clouteau, D., Cotteneau, R., Lombaert, G., 2013. Dynamics of structures coupled with elastic media—a review of numerical models and methods. *J. Sound Vib.* 332 (10), 2415–2436. doi:10.1016/j.jsv.2012.10.011.
- Colquitt, D., Brun, M., Gei, M., Movchan, A., Movchan, N., Jones, I., 2014. Transformation elastodynamics and cloaking for flexural waves. *J. Mech. Phys. Solids* 72, 131–143. doi:10.1016/j.jmps.2014.07.014.
- Polizzotto, C., 2000. A symmetric galerkin boundary/domain element method for finite elastic deformations. *Comput. Methods Appl. Mech. Eng.* 189 (2), 481–514. doi:10.1016/S0045-7825(99)00303-5.
- Farzanian, M., Arbabi, F., 2014. A pml solution for vibration of infinite beams on elastic supports under seismic loads. *J. Seismol. Earthquake Eng.* 16 (1), 1–16.
- Gaul, L., Kögl, M., M.Wagner, 2003. *Boundary Element Methods for Engineers and Scientists: An Introductory Course with Advanced Topics*, 1 Springer, Verlag Berlin Heidelberg.
- Geli, L., Bard, P., Jullien, B., 1988. The effect of topography on earthquake ground motion: a review and new results. *Bull. Seismol. Soc. Am.* 78 (1), 42–63.
- Gerdas, K., 2000. A review of infinite element methods for exterior helmholtz problems. *J. Comput. Acoust.* 8 (1), 43–62. doi:10.1016/S0218-396X(00)00004-2.
- Givoli, D., 1991. Non-reflecting boundary conditions: review article. *Geophysics* 94 (1), 1–29. doi:10.1016/0021-9991(91)90135-8.
- Hagstrom, T., Hariharan, S., 1998. A formulation of asymptotic and exact boundary conditions using local operators. *Appl. Numer. Math.* 27, 403–416.
- Hastings, F., Schneider, J., Broschat, S., 1996. Application of the perfectly matched layer (pml) absorbing boundary conditions to elastic wave propagation. *J. Acoust. Soc. Am.* 100 (5), 3061–3069. doi:10.1121/1.417118.
- Higdon, R., 1991. Absorbing boundary conditions for elastic waves. *Geophysics* 56 (2), 231–241. doi:10.1190/1.1443035.
- Hu, G., Rathsfeld, A., Yin, T., 2016. Finite element method to fluid-solid interaction problems with unbounded periodic interfaces. *Numer. Methods Partial Differ. Eq.* 32 (1), 5–35. doi:10.1002/num.21980.
- Ihlenburg, F., 1998. *Finite Element Analysis of Acoustic Scattering*. Springer, Verlag New York.
- Jones, I., Brun, M., Movchan, N., Movchan, A., 2015. Singular perturbations and cloaking illusions for elastic waves in membranes and kirchhoff plates. *Int. J. Solids Struct.* 69–70, 498–506. doi:10.1016/j.ijsolstr.2015.05.001.
- Graff, K.F., 1975. *Wave Motion in Elastic Solids*. Oxford University Press, Oxford.
- Kim, J., Kim, H., 2009. Finite element analysis of piezoelectric underwater transducers for acoustic characteristics. *J. Mech. Sci. Technol.* 23 (1), 452–460. doi:10.1007/s12206-008-1126-x.
- Komatitsch, D., Tromp, J., 2003. A perfectly matched layer absorbing boundary condition for the second-order seismic wave equation. *Geophys. J. Int.* 154 (1), 146–153. doi:10.1046/j.1365-246X.2003.01950.x.
- Kristek, J., Moczo, P., Galis, M., 2009. A brief summary of some pml formulations and discretizations for the velocity-stress equation of seismic motion. *Stud. Geophys. Geod.* 53 (1), 459–474. doi:10.1007/s11200-009-0034-6.
- Lancioni, G., 2012. Numerical comparison of high-order absorbing boundary conditions and perfectly matched layers for a dispersive one-dimensional medium. *Comput. Methods Appl. Mech. Eng.* 209–212, 74–86. doi:10.1016/j.cma.2011.10.015.
- Cremers, L., Fyfe, K., 1995. On the use of variable order infinite wave envelope elements for acoustic radiation and scattering. *J. Acoust. Soc. Am.* 97 (5–6), 2028–2040. doi:10.1121/1.411994.
- Lee, J., Tassoulas, J., 2011. Consistent transmitting boundary with continued-fraction absorbing boundary conditions for analysis of soil-structure interaction in a layered half-space. *Comput. Methods Appl. Mech. Eng.* 200 (13–16), 1509–1525. doi:10.1016/j.cma.2011.01.004.



- Leis, R., 1986. *Initial Boundary Value Problems in Mathematical Physics*. Teubner Verlag, Wiesbaden.
- Liu, G., Quek, J., 2003. A non-reflecting boundary for analyzing wave propagation using the finite element method. *Finite Element Anal. Des.* 39 (5–6), 403–417. doi:[10.1016/S0168-874X\(02\)00081-1](https://doi.org/10.1016/S0168-874X(02)00081-1).
- Lo, S., Wang, W., 2005. Generation of finite element mesh with variable size over an unbounded 2d domain. *Comput. Methods Appl. Mech. Eng.* 194 (45–47), 4668–4684. doi:[10.1016/j.cma.2004.12.011](https://doi.org/10.1016/j.cma.2004.12.011).
- Lysmer, J., Kuhlemeyer, R., 1969. Numerical comparison of high-order absorbing boundary conditions and perfectly matched layers for a dispersive one-dimensional medium. *J. Eng. Mech. Div., Proc. ASCE* 95, 859–876.
- Maier, G., Miccoli, S., Perego, U., Novati, G., 1995. Symmetric galerkin boundary element method in plasticity and gradient plasticity. *Comput. Mech.* 17 (1), 115–129. doi:[10.1007/BF00356484](https://doi.org/10.1007/BF00356484).
- Milton, G., Briane, M., Willis, J., 2006. On cloaking for elasticity and physical equations with a transformation invariant form. *New J. Phys.* 8, 248. doi:[10.1088/1367-2630/8/10/248](https://doi.org/10.1088/1367-2630/8/10/248).
- Nataf, F., 2005. New constructions of perfectly matched layers for the linearized euler equations. *C.R. Math.* 340 (10), 775–778. doi:[10.1016/j.crma.2005.04.013](https://doi.org/10.1016/j.crma.2005.04.013).
- Nataf, F., 2013. Absorbing boundary conditions and perfectly matched layers in wave propagation problems. *Radon Series on Computational and Applied Mathematics* 11, 219–231.
- Norris, A., Shuvalov, A., 2011. Elastic cloaking theory. *Wave Motion* 48 (6), 525–538. doi:[10.1016/j.wavemoti.2011.03.002](https://doi.org/10.1016/j.wavemoti.2011.03.002).
- Novati, G., Brebbia, C., 1982. Boundary element formulation for geometrically nonlinear elastostatics. *Appl. Math. Model* 6 (2), 136–138. doi:[10.1016/0307-904X\(82\)90025-7](https://doi.org/10.1016/0307-904X(82)90025-7).
- Parvanova, S., Dineva, P., Manolis, G., et al., 2014. Dynamic response of a solid with multiple inclusions under anti-plane strain conditions by the bem. *Comput. Struct.* 139, 65–83. doi:[10.1016/j.compstruc.2014.04.002](https://doi.org/10.1016/j.compstruc.2014.04.002).
- Phan-Thien, N., 1988. Rubber-like elasticity by boundary element method: finite deformation of a circular elastic slice. *Rheol. Acta* 27 (3), 230–240. doi:[10.1007/BF01329739](https://doi.org/10.1007/BF01329739).
- Polizzotto, C., 1988. An energy approach to the boundary element method. part ii: elastic-plastic solids. *Comput. Methods Appl. Mech. Eng.* 69 (3), 263–276. doi:[10.1016/0045-7825\(88\)90043-6](https://doi.org/10.1016/0045-7825(88)90043-6).
- Qi, Q., Geers, T., 1998. Evaluation of the perfectly matched layer for computational acoustics. *J. Comput. Phys.* 139 (1), 166–183. doi:[10.1002/mop.4650071304](https://doi.org/10.1002/mop.4650071304).
- Quarteroni, A., Tagliani, A., Zampieri, E., 1998. Generalized galerkin approximations of elastic waves with absorbing boundary conditions. *Comput. Methods Appl. Mech. Eng.* 163 (1–4), 323–341.
- Rappaport, C.M., 1996. Interpreting and improving the pml absorbing boundary condition using anisotropic lossy mapping of space. *IEEE Trans. Magn.* 32 (3), 968–974. doi:[10.1109/20.497403](https://doi.org/10.1109/20.497403).
- Robinovich, D., Givoli, D., Bielak, J., et al., 2011. A finite element scheme with a high order absorbing boundary condition for elastodynamics. *Comput. Methods Appl. Mech. Eng.* 200 (23–24), 2048–2066. doi:[10.1016/j.cma.2011.03.006](https://doi.org/10.1016/j.cma.2011.03.006).
- Romero, A., Tadeu, A., Galvin, P., Antonio, J., 2015. 2.5D coupled bem-fem used to model fluid and solid scattering wave. *Int. J. Numer. Methods Eng.* 101 (2), 148–164. doi:[10.1002/nme.4801](https://doi.org/10.1002/nme.4801).
- Sochacki, J., Kubichek, R., George, J., Fletcher, W., Smithson, S., 1987. Absorbing boundary conditions and surface waves. *Geophysics* 52, 60–71. doi:[10.1190/1.1442241](https://doi.org/10.1190/1.1442241).
- Song, R., Ma, J., Wang, K., 2005. The application of the non splitting perfectly matched layer in numerical modeling of wave propagation in poroelastic media. *Appl. Geophys.* 2 (4), 216–222. doi:[10.1007/s11770-005-0027-3](https://doi.org/10.1007/s11770-005-0027-3).
- Steele, C., 2001. A critical review of some traffic noise prediction models. *Applied Acoustics* 62 (3), 271–287. doi:[10.1016/S0003-682X\(00\)00030-X](https://doi.org/10.1016/S0003-682X(00)00030-X).
- Tassoulas, J., Kausel, E., 1983. Elements for the numerical analysis of wave motion in layered strata. *Int. J. Numer. Methods Eng.* 19 (7), 1005–1032. doi:[10.1002/nme.1620190706](https://doi.org/10.1002/nme.1620190706).
- Telles, J., Brebbia, C., 1979. On the application of the boundary element method to plasticity. *Appl. Math. Model* 3 (6), 466–470. doi:[10.1016/S0307-904X\(79\)80030-X](https://doi.org/10.1016/S0307-904X(79)80030-X).
- Wrobel, L., 2002. *The Boundary Element Method*, 1. Wiley, Chichester, West Sussex, England.
- Zheng, Y., Huang, X., 2002. Anisotropic perfectly matched layers for elastic waves in cartesian and curvilinear coordinates. *Earth Resour. Lab. Ind. Consortia* 1–18.
- Sacks, Z.S., Kingsland, D.M., Lee, R., Lee, J-F., 1995. A perfectly matched anisotropic absorber for use as an absorbing boundary condition. *IEEE Trans. Antennas Propagation* 43 (12), 1460–1463. doi:[10.1109/8.477075](https://doi.org/10.1109/8.477075).